


# Pathogen-Associated Molecules from Gut Translocation Enhance Severity of Cecal Ligation and Puncture Sepsis in Iron-Overload $\beta$ -Thalassemia Mice

This article was published in the following Dove Press journal:  
*Journal of Inflammation Research*

Kritsanawan Sae-khow<sup>1</sup>  
Awirut Charoensappakit<sup>2</sup>  
Peerapat Visitchanakun<sup>1</sup>  
Wilasinee Saisorn<sup>2</sup>   
Saovaros Svasti<sup>3</sup>  
Suthat Fucharoen<sup>3</sup>  
Asada Leelahavanichkul<sup>2,4</sup>

<sup>1</sup>Medical Microbiology, Interdisciplinary and International Program, Graduate School, Chulalongkorn University, Bangkok, Thailand; <sup>2</sup>Translational Research in Inflammation and Immunology Research Unit (TRIRU), Department of Microbiology, Chulalongkorn University, Bangkok, Thailand; <sup>3</sup>Thalassemia Research Center, Institute of Molecular Biosciences, Mahidol University, Nakhonpathom, Thailand; <sup>4</sup>Department of Microbiology, Faculty of Medicine, Chulalongkorn University, Bangkok, Thailand

**Introduction:** Systemic inflammation induced by gut translocation of lipopolysaccharide (LPS), a major component of Gram-negative bacteria, in thalassemia with iron-overload worsens sepsis. However, the impact of (1 $\rightarrow$ 3)- $\beta$ -D-glucan (BG), a major fungal molecule, in iron-overload thalassemia is still unclear. Hence, the influence of BG was explored in 1) iron-overload mice with sepsis induced by cecal ligation and puncture (CLP) surgery; and 2) in bone marrow-derived macrophages (BMMs).

**Methods:** The heterozygous  $\beta$ -globin-deficient mice, Hbb<sup>th3/+</sup> mice, were used as representative thalassemia (TH) mice. Iron overload was generated by 6 months of oral iron administration before CLP surgery- induced sepsis in TH mice and wild-type (WT) mice. Additionally, BMMs from both mouse strains were used to explore the impact of BG.

**Results:** Without sepsis, iron-overload TH mice demonstrated more severe intestinal mucosal injury (gut leakage) with higher LPS and BG in serum, from gut translocation, when compared with WT mice. With CLP in iron-overload mice, sepsis severity in TH mice was more severe than WT as determined by survival analysis, organ injury (kidney and liver), bacteremia, endotoxemia, gut leakage (FITC-dextran) and serum BG. Activation by LPS plus BG (LPS+BG) in BMMs and in peripheral blood-derived neutrophils (both WT and TH cells) demonstrated more prominent cytokine production when compared with LPS activation alone. In parallel, LPS+BG also prominently induced genes expression of M1 macrophage polarization (*iNOS*, *TNF- $\alpha$*  and *IL-1 $\beta$* ) in both WT and TH cells in comparison with LPS activation alone. In addition, LPS+BG activated macrophage cytokine production was enhanced by a high dose of ferric ion (800 mM), more predominantly in TH macrophages compared with WT cells. Moreover, LPS+BG induced higher glycolysis activity with similar respiratory capacity in RAW264.7 (a macrophage cell line) compared with LPS activation alone. These data support an additive pro-inflammatory effect of BG upon LPS.

**Conclusion:** The enhanced-severity of sepsis in iron-overload TH mice was due to 1) increased LPS and BG in serum from iron-induced gut-mucosal injury; and 2) the pro-inflammatory amplification by ferric ion on LPS+BG activation.

**Keywords:** thalassemia, iron overload, leaky-gut, sepsis

Correspondence: Asada Leelahavanichkul  
Translational Research in Inflammation and Immunology Research Unit (TRIRU),  
Department of Microbiology, Chulalongkorn University, Bangkok 10330, Thailand  
Tel +66-2-256-4251  
Fax +66-2-252-6920  
Email aleelahavanit@gmail.com

## Introduction

$\beta$ -thalassemia is one of the most common inherited disorders of hemoglobin synthesis in Asia caused by the point mutations of the  $\beta$ -globin gene that induces  $\beta$ -globin deficiency.<sup>1</sup> Red blood cell with  $\beta$ -globin deficiency induces ineffective

erythropoiesis, failure or premature death of erythroid progenitor cells, leads to hemolytic anemia, iron-overload, splenomegaly, and abnormal bone growth.<sup>1-3</sup> Indeed, iron-overload (secondary hemochromatosis) is common in  $\beta$ -thalassemia mainly due to the required regular blood transfusions<sup>4</sup> and increases susceptibility to infection. Overburden of iron is directly toxic to immune cells resulting in worse bactericidal activity and also enhances micro-organism growth.<sup>5,6</sup> In addition, iron-overload induces permeability defect of intestinal mucosa as determined by gut translocation of lipopolysaccharide (LPS), a major component of Gram-negative bacteria in gut,<sup>7,8</sup> that induces systemic inflammation<sup>9-11</sup> and increased incidence of Gram-negative bacteremia in patients.<sup>12</sup> Unsurprisingly, iron-overload is a risk factor of bacteremia of patients with thalassemia.<sup>13</sup> Because of the increased sepsis severity in pre-existing inflammatory conditions<sup>14-16</sup> and iron-overload in TH mice enhanced gut translocation of LPS,<sup>17</sup> iron-overload TH mice are more susceptible to LPS sepsis model.<sup>17</sup> However, some important aspects of human sepsis are different from the LPS injection model including non-bacteremia and too much cytokine production as the LPS model is categorized as a non-infectious systemic inflammation model.<sup>18,19</sup> In contrast, the cecal ligation and puncture (CLP) sepsis model more closely resembles human sepsis, particularly in disease pathophysiology (clinical course, bacteremia, and cytokine levels).<sup>20</sup>

Although the impact of serum LPS originating from gut translocation in iron-overload TH mice as a systemic inflammatory inducer is demonstrated,<sup>17</sup> the major organismal molecules in gut consist of not only LPS from Gram-negative bacteria, but also (1 $\rightarrow$ 3)- $\beta$ -D-glucan (BG) from gut fungi.<sup>11</sup> We have demonstrated the synergistic influence of LPS with BG due to gut translocation in several models.<sup>9,21-23</sup> Hence, it is possible that the impact of LPS together with BG from gut translocation in the condition of iron-overload in TH mice is interesting. Although fungi in mice gut are not prominent in comparison with humans,<sup>24</sup> gut translocation of BG into blood circulation are mentioned in mouse models.<sup>11,25</sup> Indeed, the synergistic effect of BG upon LPS activation through the combined signaling between Dectin-1 and TLR-4, a main pattern recognition receptor of BG and LPS, respectively, has been demonstrated.<sup>26,27</sup> Moreover macrophage  $\beta$ -globin is induced by LPS<sup>28</sup> possibly to counteract the iron metabolites during bactericidal activity,<sup>29</sup> the reduced  $\beta$ -globin gene expression in TH macrophages

enhanced reactive oxygen species related cell-injury is demonstrated.<sup>17</sup> However, the influence of LPS+BG in iron-overload TH mice has never been tested. Here, we hypothesize that iron-overload in thalassemia causes translocation of organismal molecules from gut and induces sepsis susceptibility. We tested the hypothesis with CLP sepsis model, a model that closely resembles human sepsis,<sup>18,19</sup> in Hbb<sup>th3/+</sup> (heterozygous  $\beta$ -globin knockout) mice after 6 months of iron administration in comparison with WT mice.

## Materials and Methods

### Animal and Animal Models

Animal study protocol was approved by the Institutional Animal Care and Use Committee of the Faculty of Medicine, Chulalongkorn University, Bangkok, Thailand (SST 04/2561), based upon the National Institutes of Health (NIH), USA. Thalassemia (TH) mice were heterozygous  $\beta$ -globin knockout mice (Hbb<sup>th3/+</sup> mice) on C57BL/6 background that were obtained from Mahidol University, Thailand.<sup>30</sup> Wild-type (WT) C57BL/6 mice were purchased from the National Laboratory Animal Center, Nakhornpathom, Thailand. The iron-overload model was performed by oral administration of iron sucrose (Venofer, USP) at 10 mg/dose three times per week in male, 8-week-old mice, for 6 months as modified from a previous study.<sup>17</sup> In control mice, the same volume of normal saline solution (NSS) was administered. To explore the impact of iron-overload in mice, blood samples were collected through cardiac puncture under isoflurane anesthesia at sacrifice. In parallel, internal organs including kidney, liver, spleen, and intestine (cecum) were collected and fixed in 10% formalin for histology, put in Cryogel (Leica Biosystems, Richmond, IL, USA) for immunofluorescent staining and kept at  $-80^{\circ}\text{C}$  for determination of iron in internal organs.

In addition, the cecal ligation and puncture sepsis model or sham surgery was performed following previous studies.<sup>31,32</sup> Briefly, cecum was ligated at 10 mm from the cecal tip, through mid-abdominal incision and punctured twice with a 21-gauge needle. Fentanyl at a dose of 0.03 mg/kg in 100 mL NSS was administered subcutaneously for the postoperative analgesia and fluid replacement after operation, at 6 hours and 24 hours later. In the sham operation, cecum was identified before closing the abdominal wall. Mice were sacrificed by cardiac puncture under isoflurane anesthesia at 18 hours or after 96 hours post CLP for sample collection and survival analysis, respectively.

## Mouse Blood Sample Analysis and Iron Measurement

To determine white blood cell (WBC) count from peripheral blood, 15  $\mu$ L of blood was mixed with 250  $\mu$ L of 3% acetic acid, a hemolytic solution, and the total number of leukocytes was counted with a hemocytometer. Meanwhile, 10  $\mu$ L of blood was smeared on a glass slide for Wright stain and counted with x100 magnification in 20 fields to determine the percentage of polymorphonuclear cells (PMN) and monocyte. The total number of PMN was calculated by total leukocyte count from hemocytometer multiplied by the percentage of cells from the Wright stain glass slide.<sup>33</sup>

A micro-hematocrit method with a Hitachi 917 automated biochemistry analyzer (Roche Diagnostics, Indianapolis, IN, USA) was used for hematocrit (Hct) measurement. Meanwhile, BioAssay Systems (Haywood, CA, USA) was used for serum creatinine (Scr) (DICT-500), blood urea nitrogen (BUN) (DIUR-500), aspartate transaminase (AST) (EASTR-100), and alanine transaminase (ALT) (EALT-100). Serum cytokines were measured by enzyme-linked immunosorbent assay (ELISA) (PeproTech, NJ, USA). To determine blood bacterial burdens, mouse blood samples in several dilutions were directly spread onto blood agar plates (Oxoid, Hampshire, UK) and incubated at 37°C for 24 hours before enumeration of bacterial colonies. In addition, endotoxin (LPS) in serum was evaluated as a sepsis parameter using HEK-Blue LPS Detection Kit 2 (InvivoGen, San Diego, CA, USA).<sup>34</sup> Values less than 0.01 EU/mL were recorded as 0 due to the lower limit of the test. For organ iron accumulation, the organs including kidney, liver, spleen, and intestine (cecum) were washed several times in phosphate buffer solution (PBS), weighed, homogenized and centrifuged for the determination of ferric ion in supernatant as the representative of tissue iron accumulation by iron assay (Ab83366, Abcam, Cambridge, UK). Of note, cecum is an intestinal part with the highest abundance of fungi,<sup>35</sup> endogenous sources of (1 $\rightarrow$ 3)- $\beta$ -D-glucan (BG), an organismal molecule of interest.

## Gut Leakage Determination

Intestinal permeability defect was determined by the detection of fluorescein isothiocyanate dextran (FITC-dextran), a nonabsorbable high-molecular-weight molecule, in serum after an oral administration of 12.5 mg FITC-dextran (molecular mass, 4.4 kDa) (FD4; Sigma-

Aldrich, St. Louis, MO, USA) at 3 hours prior to sacrifice. Then, FITC-dextran in serum was measured by Fluorospectrometer (NanoDrop 3300; Thermo Fisher Scientific, Wilmington, DE, USA).<sup>34</sup> In parallel, spontaneous serum elevation of BG, a major cell-wall component of gut fungi was measured by Fungitell assay (Associates of Cape Cod, Falmouth, MA, USA) and values less than 7.8 pg/mL were recorded as 0 due to the lower limit of the test.<sup>34</sup>

## Histological Analysis and Immunofluorescent Stain

Internal organs were fixed in 10% neutral formalin for 72 hours before embedding in paraffin-blocks. The staining by Prussian blue with hematoxylin and eosin (H&E) color was performed in 4  $\mu$ m-thick paraffin-sections to detect iron accumulation in organs following a previous study.<sup>36</sup> Briefly, the sections were immersed in 20% hydrochloric acid with 10% potassium ferrocyanide for 20 minutes before washing with distilled water and counterstained by H&E color (hematoxylin for 6 minutes and eosin for 1 minute). After that the sections were dehydrated in increasing alcohol gradients and cleared in Xylene before mounting cover glasses with Resinous Mounting Medium. All reagents were purchased from Sigma-Aldrich. The area of blue-colored iron staining was counted against the total area by ImageJ (NIH, Bethesda, MD, USA). For kidney histology, the semi-quantitative score of tubular damage at cortex and medulla was defined as tubular epithelial swelling, vacuolization, necrosis, and desquamation at 200x magnification from five randomly selected fields per slide, as follows: 0, normal; 1, damage <25% of area; 2, damage 25–50% of area; 3, damage 50–75% of area; and 4, damage >75% of area.<sup>37</sup> On the other hand, the area of liver injury was defined as hepatocyte swelling, sinusoidal congestion, vacuolization, perivascular inflammation and immune cells infiltration as in the scoring system mentioned above modified from previous studies.<sup>38,39</sup> Because of the high abundance of fungi in cecum,<sup>35</sup> only cecal tight junctions were evaluated. Then, cecum in Cryogel (Leica Biosystems, Richmond, IL, USA) were cut into 5  $\mu$ m-thick frozen sections, fixed in acetone, blocked by blocking buffer and stained with primary fluorescent antibody against enterocyte tight junction molecules including Occludin-1, Claudin-1 or Zona occludens 1 (ZO-1) and secondary antibodies in green, Alexa Fluor 488 (Life Technologies, Carlsbad, CA, USA). Then,

by ZEISS LSM 800 (Carl Zeiss, Germany) was used for the visualization.

## Macrophage Functions (Cytokine Production, Microbicidal Activity, Macrophage Polarization and Extra Cellular Flux Analysis)

A protocol for bone marrow (BM)-derived macrophage preparation from femur was followed.<sup>21,40</sup> In brief, BM cells were incubated in supplemented Dulbecco's Modified Eagle Medium (DMEM) with macrophage-colony stimulating factor (M-CSF) from 20% conditioned medium of L929 cell line in a 5% CO<sub>2</sub> incubator at 37°C for 7 days before harvesting with cold PBS and then examined for macrophage phenotype by flow cytometry analysis with Anti-F4/80 and anti-CD11c antibody (BioLegend, San Diego, CA, USA). Then a high dose (800 µM/well) of ferric chloride (FeCl<sub>3</sub>) (Sigma-Aldrich, St. Louis, MO, USA) was added into the activation by endotoxin (LPS of *Escherichia coli* 026:B6, Sigma-Aldrich) at 100 ng/mL with or without CM-Pachyman (BG) (Megazyme, Bray, Ireland, UK), a representative of BG, at 10 µg/mL with macrophages (1×10<sup>5</sup> cells/well) for 6 h before supernatant cytokines determination by ELISA assay (PeproTech, NJ, USA) or macrophage bactericidal activity.<sup>41,42</sup> Briefly, bactericidal activity was evaluated by incubating *E. coli* (American Type Culture Collection, ATCC, Manassas, VA, USA) at 1×10<sup>7</sup> colony forming unit (CFU) with 25 µL of normal mouse serum (as an opsonin) into the activated macrophages (1×10<sup>5</sup> cell/well) as in the above conditions for 15 minutes. After that, the non-phagocytized bacteria were washed, eradicated by gentamicin (Sigma-Aldrich) 100 µg/mL (100 µL/well), and further incubated for 1 hour before cell lysis induction by 200 µL of sterile water/well and plating onto Tryptic soy agar (TSA) (Oxoid, Hampshire, UK) in serial dilution. Bacterial count was evaluated after 24 hours of 37°C incubation. Macrophage killing activity is inversely correlated with the enumerated bacterial colonies.

Because of the iron-overload induced pro-inflammatory macrophage polarization,<sup>43</sup> the gene expression of macrophage polarization by quantitative polymerase chain reaction (qPCR) was examined after 6 hours of the activations following a previous study.<sup>41</sup> In brief, total RNA was prepared by Trizol (Thermo Fisher Scientific, Waltham, MA, USA), quantified by Nano drop ND-1000 (Thermo Fisher Scientific) and RNA was converted into cDNA by Reverse Transcription System and quantitative polymerase chain

reaction (qPCR) using SYBR Green master mix (Applied Biosystems, Thermo Fisher Scientific), cDNA template and target primers based on  $\Delta\Delta CT$  method. The sequences of primers for M1 macrophage polarization (*iNOS*, *TNF- $\alpha$*  and *IL-1 $\beta$* ) and M2 macrophage polarization (*Arginase-1*, *FIZZ* and *TGF- $\beta$* ) (Integrated DNA Technologies, Coralville, IA, USA) normalized by the expression of house-keeping gene  *$\beta$ -actin* were used (Table 1).

Moreover, iron in macrophages is utilized as a cofactor in many pathways that regulate energy production.<sup>44</sup> Hence, energy metabolism profiles of macrophages were estimated through glycolysis and mitochondrial oxidative phosphorylation with extracellular acidification rate (ECAR) and oxygen consumption rate (OCR), respectively, by Seahorse XFp Analyzers (Agilent, Santa Clara, CA, USA). Because of the technical difficulties in the extracellular flux analysis, macrophage cell line RAW264.7 (ATCC TIB-71), but not bone marrow-derived macrophages, was used. As such, RAW264.7 at 1×10<sup>4</sup> cells/well were activated by FeCl<sub>3</sub> (800 µM/well) with LPS (100 ng/mL) with or without BG (10 µg/mL) for 6 hours before determination of the extracellular flux analysis using Seahorse Wave 2.6 software as previously described.<sup>41</sup> Glycolysis and mitochondrial parameters were calculated with generator program-report of XF test based on the following equations;

- Glycolysis = ECAR between glucose and oligomycin – ECAR before glucose administration;
- Glycolysis capacity = CAR between oligomycin and 2-Deoxy-d-glucose (2-DG) – ECAR before glucose administration;
- Glycolysis reserve = ECAR between oligomycin and 2-DG – ECAR between glucose and oligomycin;
- Basal respiration = OCR before oligomycin – OCR after antimycin A/rotenone;
- Respiratory capacity (maximal respiration) = OCR between Carbonyl cyanide-4-(trifluoromethoxy)-phenylhydrazone (FCCP) and antimycin A/rotenone – OCR after antimycin A/rotenone; and
- Respiratory reserve = OCR between FCCP and antimycin A/rotenone – OCR before oligomycin.

## Neutrophil Functions (Cytokine Production and Chemotaxis)

Neutrophil was isolated from heparinized blood collected from cardiac puncture under isoflurane anesthesia



**Table 1** List of Primers

Primers		
Inducible nitric oxide synthase ( <i>iNOS</i> )	Forward	5'-CCCTTCCGAAGTTTCTGGCAGCAGC-3'
	Reward	5'-GGCTGTCAGAGCCTCGTGGCTTTG-3'
Arginase 1 ( <i>Arg-1</i> )	Forward	5'-CAGAAGAATG GAAGAGTCAG-3'
	Reward	5'-CAGATATGCA GGA GTACAC-3'
Tumor necrosis factor $\alpha$ ( <i>TNF-<math>\alpha</math></i> )	Forward	5'-CCTCACACTCAGATCATCTTCTC-3'
	Reward	5'-AGATCCATGCCG TTGGCCAG-3'
Interleukin-1 $\beta$ ( <i>IL-1<math>\beta</math></i> )	Forward	5'-GAAATGCCACCTTTTGACAGTG-3'
	Reward	5'-TGGATGCTCTCATCAGGACAG-3'
Resistin-like molecule- $\alpha$ ( <i>FIZZ-1</i> )	Forward	5'-GCCAGGTCTGGAACCTTTC-3'
	Reward	5'-GGAGCAGGGAGATGCAGATGAG-3'
Transforming growth factor- $\beta$ ( <i>TGF-<math>\beta</math></i> )	Forward	5'-CAGAGCTGCGCTTGACAGAG-3'
	Reward	5'-GTCAGCAGCCGGTTACCAAG-3'
$\beta$ -actin	Forward	5'-CGGTTCCGATGCCCTGAGGCTCTT-3'
	Reward	5'-CGTCACACTTCATGATGGAATTGA-3'

of 8-week-old WT and TH mice modified from previous studies.<sup>45,46</sup> Briefly, 1 mL of blood was put in 3 mL of Ficoll-Paque Polymorphep (Axis-Shield, Dundee, UK) to separate layers of PMN cells. Subsequently, isolated PMN cells were washed by equal volume of PBS at 1500 rpm for 5 minutes and contaminated red blood cells were lysed by 0.15 M ammonium chloride (NH<sub>4</sub>Cl) solution (Merck KGaA, Darmstadt, Germany) for 5 minutes at room temperature. Then, isolated PMN cells were washed by PBS again before incubation with 1 mL of DMEM.<sup>47</sup> More than 97% of the cells derived by this protocol had morphological characteristics of poly-morphonuclear cells by Diff-Quick staining. Then the resuspended neutrophils were incubated at 37°C in a 5% CO<sub>2</sub> incubator and incubated with FeCl<sub>3</sub> (800  $\mu$ M/well) with LPS (100 ng/mL) with or without BG (10  $\mu$ g/mL) for 6 hours before determination of supernatant cytokines (PeproTech).

In addition, neutrophil chemotaxis was evaluated by the migration of neutrophils through permeable support using the transwell assay (Millipore, Burlington, MA, USA) with a 3  $\mu$ m pore-size filter following a previous study.<sup>47</sup> In brief, neutrophils at 1 x 10<sup>6</sup> cells were seeded into the upper chamber, while the previously described conditions of N-formyl-methionyl-leucyl-phenylalanine (fMLP) (Sigma-Aldrich), a chemoattractant positive control, at 100  $\mu$ M were added into the lower chamber and incubated at 37°C in 5% CO<sub>2</sub> for 120 minutes. Finally, the migrated neutrophils in each well were counted by an automated cell counter (Countess™ II, Thermo Fisher Scientific).

## Statistical Analysis

All data were analyzed by Statistical Package for Social Sciences software (SPSS 22.0, IBM Corporation, Armonk, NY, USA) and Graph Pad Prism version 7.0 software (La Jolla, CA, USA). Results are presented as mean  $\pm$  standard error (SE). Survival analyses were evaluated with the Log rank test. The differences between groups were examined for statistical significance by one-way analysis of variance (ANOVA) followed by Tukey's analysis or Student's *t*-test for comparisons of multiple or two groups, respectively and *p* < 0.05 was considered statistically significant.

## Results

Iron-overload-induced secondary hemochromatosis in several organs and gastro-intestinal mucosal permeability defect (gut leakage), were more predominant in thalassemia (TH) mice. Gut leakage in TH mice enhanced gut translocation LPS and BG from Gram negative bacteria and fungi, respectively, into systemic circulation that induced systemic inflammation and enhanced sepsis severity.

## Prominent Iron-Overload and Intestinal Barrier Defect in Iron-Administered Thalassemia Mice Enhanced Severity of Cecal Ligation and Puncture

Iron administration for 6 months in TH mice did not improve anemia (Figure 1A) but prominently elevated liver enzymes (Figure 1B). Iron accumulation in several internal organs including kidney, spleen, liver, and intestine in TH mice was higher than wild-type (WT) mice as

determined by total iron measurement and Prussian blue staining (Figure 1C–G). Meanwhile, iron accumulation could not be demonstrated in both strains of mice without iron gavage (Figure 1C–G). In parallel, iron induced intestinal tight junction injury in both WT and TH mice but was more severe in iron-overload TH mice as demonstrated by the reduction of tight junction molecules (Occludin-1, Claudin-1 and ZO-1) (Figure 2A–D) together with gut leakage (FITC-dextran assay) and gut translocation of LPS and BG into serum (Figure 2E–G). These data supported the more severe complications from iron accumulation in TH mice.<sup>8,9,11</sup>

Although the increased susceptibility to infection of patients with TH is well-known,<sup>13</sup> it is still unclear if the effect is due to iron-overload or the immunity defect. Sepsis severity in TH mice without iron accumulation did not differ from non-iron WT mice as determined by survival analysis, leukopenia, neutropenia, monocyte count, renal injury (BUN and Scr), liver damage (AST and ALT), bacteremia, endotoxemia, gut leakage (FITC-dextran and serum BG), and serum cytokines (Figure 3A–O). Additionally, histological damage of kidney and spleen was not different between CLP mice with or without iron-overload while liver histology in TH was more severe than WT in iron-overload condition (Figure 4A–C). With iron gavage, there were brown dots of iron in liver and spleen in both WT and TH mice but iron in proximal renal tubules was detectable only in TH mice (Figure 4C, inset pictures) supporting the higher iron accumulation in TH mice. Then the more severe iron toxicity in iron-overload TH mice compared with WT without sepsis (sham) was demonstrated by liver injury (ALT), gut-leakage (FITC-dextran and serum BG), and serum pro-inflammatory cytokines (TNF- $\alpha$  and IL-6), but not renal injury (Figure 3F, K–N), supporting that pre-existing inflammation induced more severe sepsis as previously described.<sup>9–11,22,34,48</sup> Unsurprisingly, iron-overload TH mice demonstrated more severe sepsis as evaluated by the several sepsis parameters (mentioned above) in comparison with WT mice (Figure 3A–O). Of note, baseline leukocyte count in peripheral blood and sepsis-induced neutropenia (without iron gavage) were not different between WT and TH mice, however neutropenia in sepsis with iron gavage of TH mice was more severe than WT (Figure 3B–D).

## Iron and Organismal Molecules Enhance Inflammatory Responses of Innate Immune Cells, an Enhanced Inflammation in Iron-Overload Thalassemia Mice

Systemic cytokines induced from LPS and BG in serum from gut leakage in iron-overload TH mice was demonstrated both before and after CLP surgery due to gut mucosal injury by iron-overload (Figure 2E–G) and sepsis (Figure 3G–L), respectively. Hence, iron and organismal molecules might have an impact upon inflammatory responses. Without ferric ion, BG alone did not stimulate macrophages while BG enhanced LPS-activated cytokine production in both WT and TH macrophages (Figure 5A–C). Although ferric ion alone only slightly activated macrophage cytokines in both WT and TH, ferric ion enhanced the responses against LPS or LPS+BG in TH macrophages (Figure 5A–C) possibly due to  $\beta$ -globin gene defect-induced iron toxicity.<sup>17</sup> In addition, bactericidal activity, as evaluated by the viability of phagocytized bacteria, was improved by either ferric ion or any organismal molecules (LPS, BG and LPS+BG) and the activity of combined ferric ion with organismal molecules did not change the activity in both WT and TH cells (Figure 5D).

Moreover, impact of these activations upon macrophage polarization<sup>49</sup> was explored. Accordingly, LPS+BG increased expression of M1 macrophage polarization (*iNOS*, *TNF- $\alpha$*  and *IL-1 $\beta$* ) compared with the activation by LPS alone and ferric ion enhanced the expression of these genes in both macrophages from WT and TH mice (Figure 6A–C). In comparison with WT macrophages, ferric ion in LPS+BG vs LPS activation in TH macrophages induced high expression of *TNF- $\alpha$*  and *IL-1 $\beta$*  versus only *TNF- $\alpha$*  alone, respectively (Figure 6B and C). In contrast, gene expression of M2 macrophage polarization was not changed (Figure 6D–F). Furthermore, impact of ferric ion on LPS and LPS+BG upon cell-energy was determined by extracellular flux analysis due to the importance of iron in macrophage energy-regulation.<sup>44</sup> Because of the technical difficulty in using primary cells for the extracellular flux analysis, a macrophage cell line, RAW264.7, was used. As such, LPS+BG reduced mitochondria function (respiratory capacity and reserve), but increased glycolysis activity (glycolysis, glycolysis capacity and reserve), in comparison with control macrophages and the addition of ferric ion decreased both respiratory capacity and glycolysis activity (Figure 6G–M). Of note, induction with LPS also demonstrated the similar responses to LPS+BG, including ferric

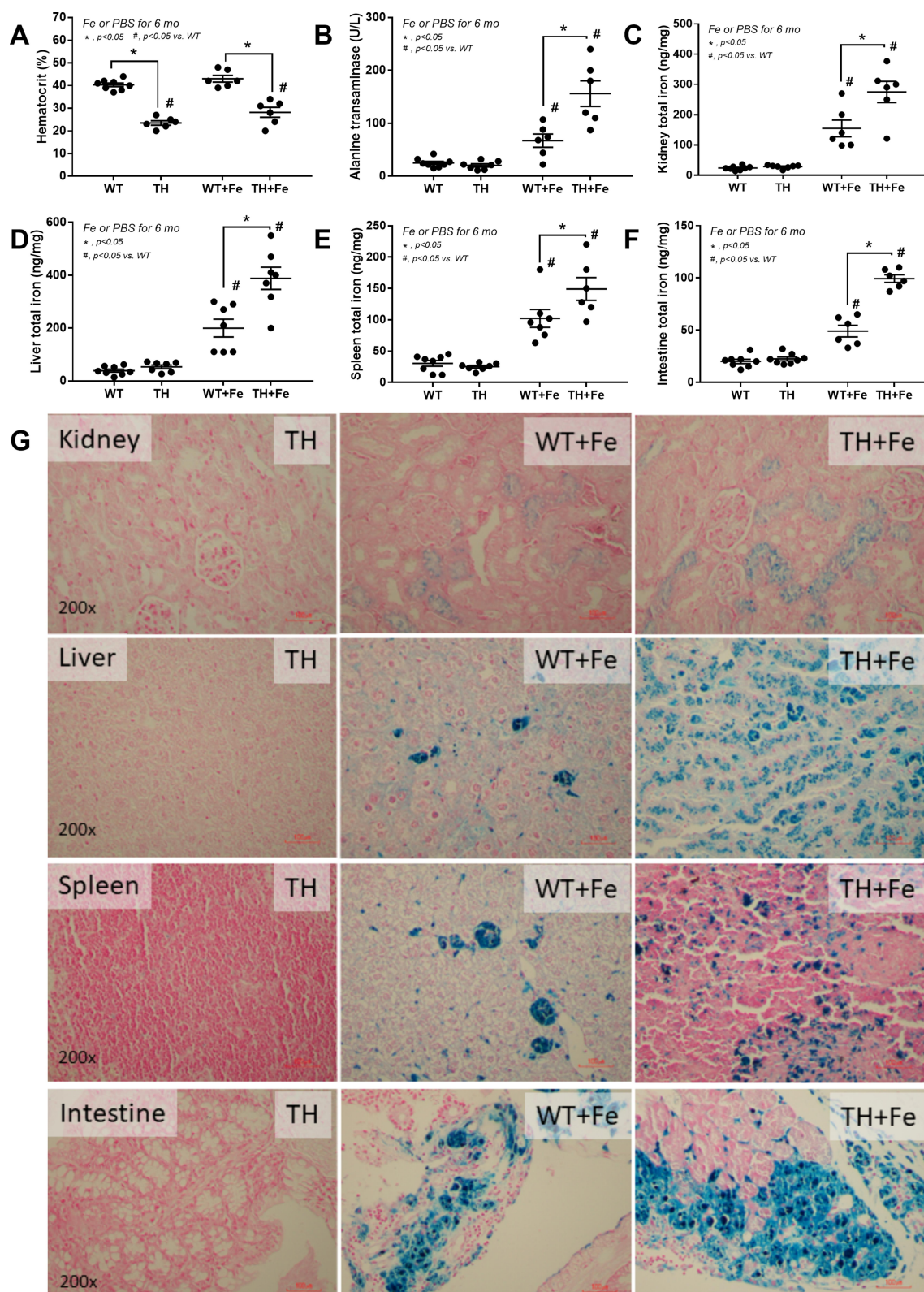


**Figure 1** Characteristics of wild-type (WT) and thalassemia (TH) mice with or without iron-overload as determined by hematocrit (A), serum alanine transaminase (B), iron measurement in several organs (C–F) and representative figures of iron accumulation in organs as stained by Prussian blue color (G) are demonstrated ( $n = 6-8$ /group for A–F). Only control TH mice are demonstrated due to the similarity between WT and TH in the control group. \* $p < 0.05$ ; # $p < 0.05$  vs. WT.



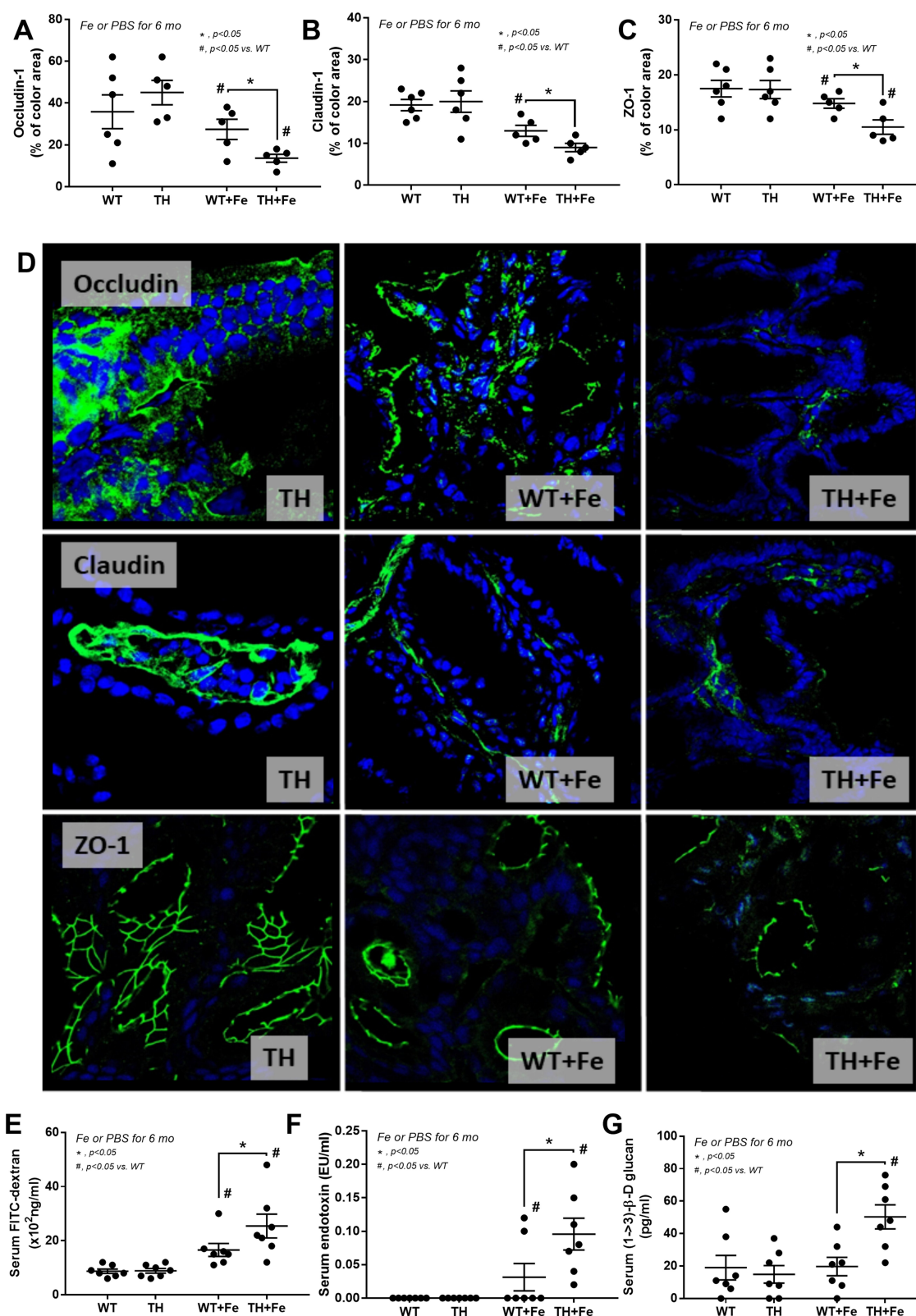


**Figure 2** Tight junction injury as determined by abundance score of intestinal tight junction proteins including Occludin-1, Claudin-1 and Zonula occludens-1 (ZO-1) with immunofluorescence (**A–C**) ( $n = 5–6$ /group) and representative figures (original magnification was 400 $\times$ ) (**D**) in wild-type (WT) and thalassemia (TH) mice with or without iron-overload are demonstrated. Only figures of control TH mice are demonstrated due to the similarity between WT and TH in the control group. In addition, gut permeability defect by FITC-dextran assay (**E**), endotoxemia (**F**), and serum (1 $\rightarrow$ 3)- $\beta$ -D-glucan (BG) (**G**) ( $n = 6–8$ /group for **E–G**) are demonstrated. \* $p < 0.05$ ; # $p < 0.05$  vs. WT.



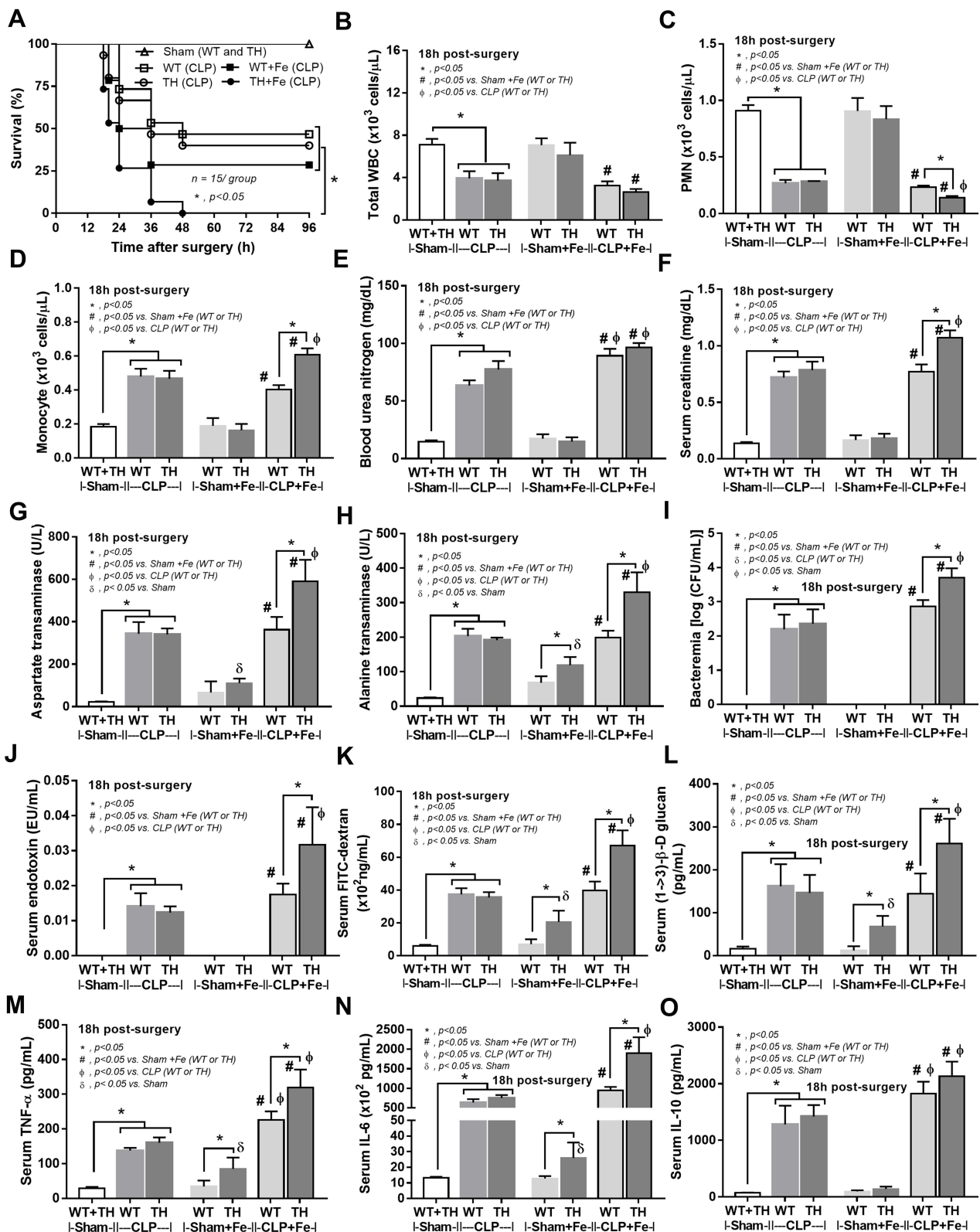


**Figure 3** Severity of sepsis in wild-type (WT) and thalassemia (TH) mice with or without iron-overload with sham or cecal ligation and puncture (CLP) surgery as determined by survival analysis (**A**), peripheral blood smear analysis including total white blood cells (WBC), polymorphonuclear cells (PMN) and monocyte count from (**B–D**), renal injury by blood urea nitrogen and serum creatinine (**E** and **F**), liver damage by aspartate transaminase and alanine transaminase (**G** and **H**), blood bacterial burdens by bacteremia and endotoxemia (**I** and **J**), gut leakage by serum FITC-dextran and serum (1 $\rightarrow$ 3)- $\beta$ -D-glucan (**K** and **L**) and serum cytokines (**M–O**) are demonstrated (n = 6–12/group). Sham data from WT and TH were combined due to the similar value between WT and TH mice. \*p < 0.05; #p < 0.05 vs Sham+Fe (WT or TH);  $\phi$ p < 0.05 vs CLP (WT or TH);  $\delta$ p < 0.05 vs Sham.

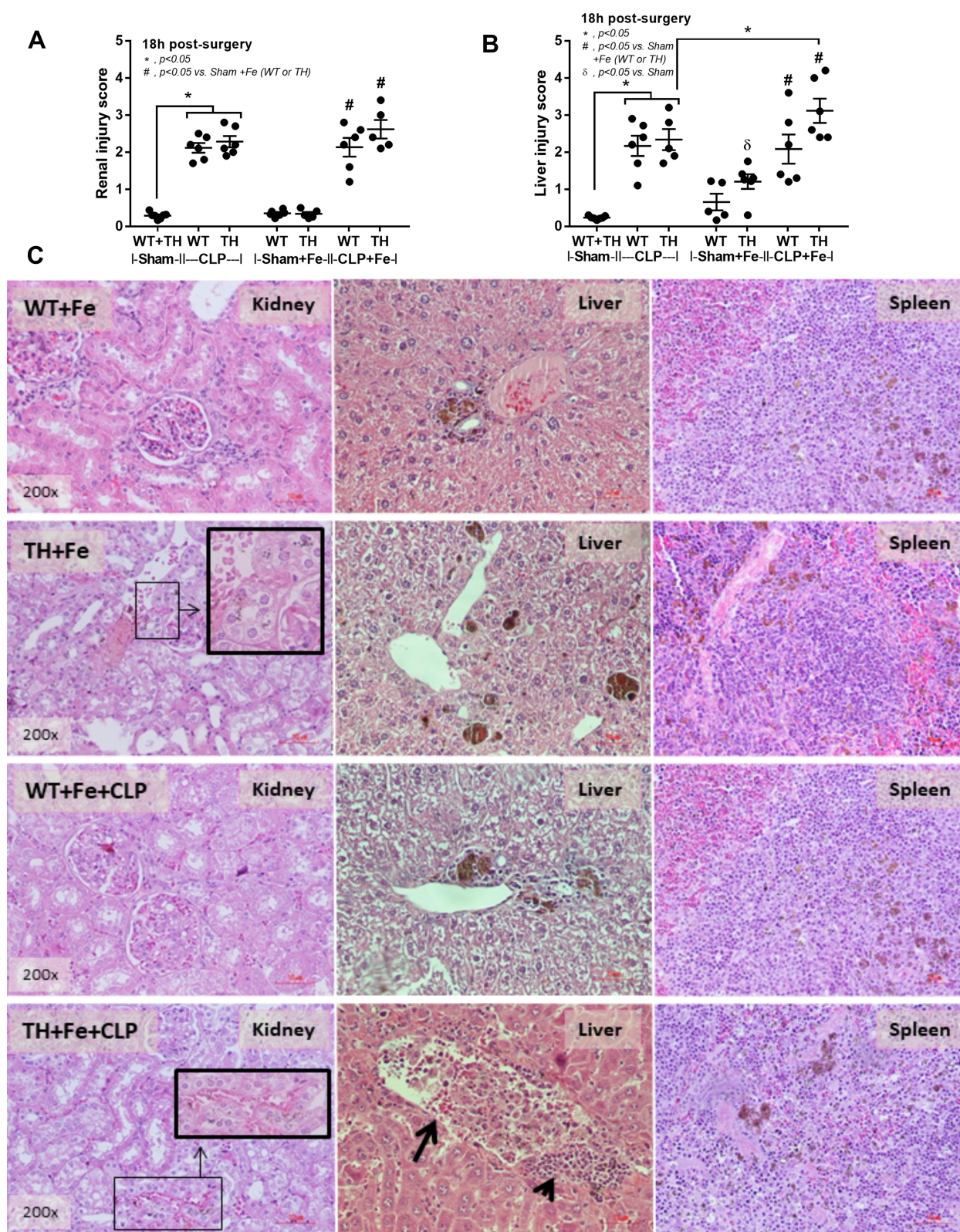


**Figure 4** Damage score in kidney and liver from wild-type (WT) and thalassemia (TH) mice with or without iron-overload with sham or cecal ligation and puncture (CLP) surgery (**A** and **B**) ( $n = 5-7/\text{group}$ ) (sham data from WT and TH were combined due to the similar value between WT and TH mice). Additionally, representative pictures of hematoxylin and eosin staining from kidney, liver and spleen (**C**) are demonstrated (only pictures of mice with iron administration are shown). Of note, the brown color is the staining color of iron and inset pictures demonstrate the magnification of brown dot iron accumulation in proximal tubular cells. Arrowhead, inflammatory cells accumulation; Arrow, sinusoidal dilatation with inflammatory cells infiltration;  $*p < 0.05$ ;  $^{\#}p < 0.05$  vs Sham+Fe (WT or TH);  $^{\delta}p < 0.05$  vs Sham.



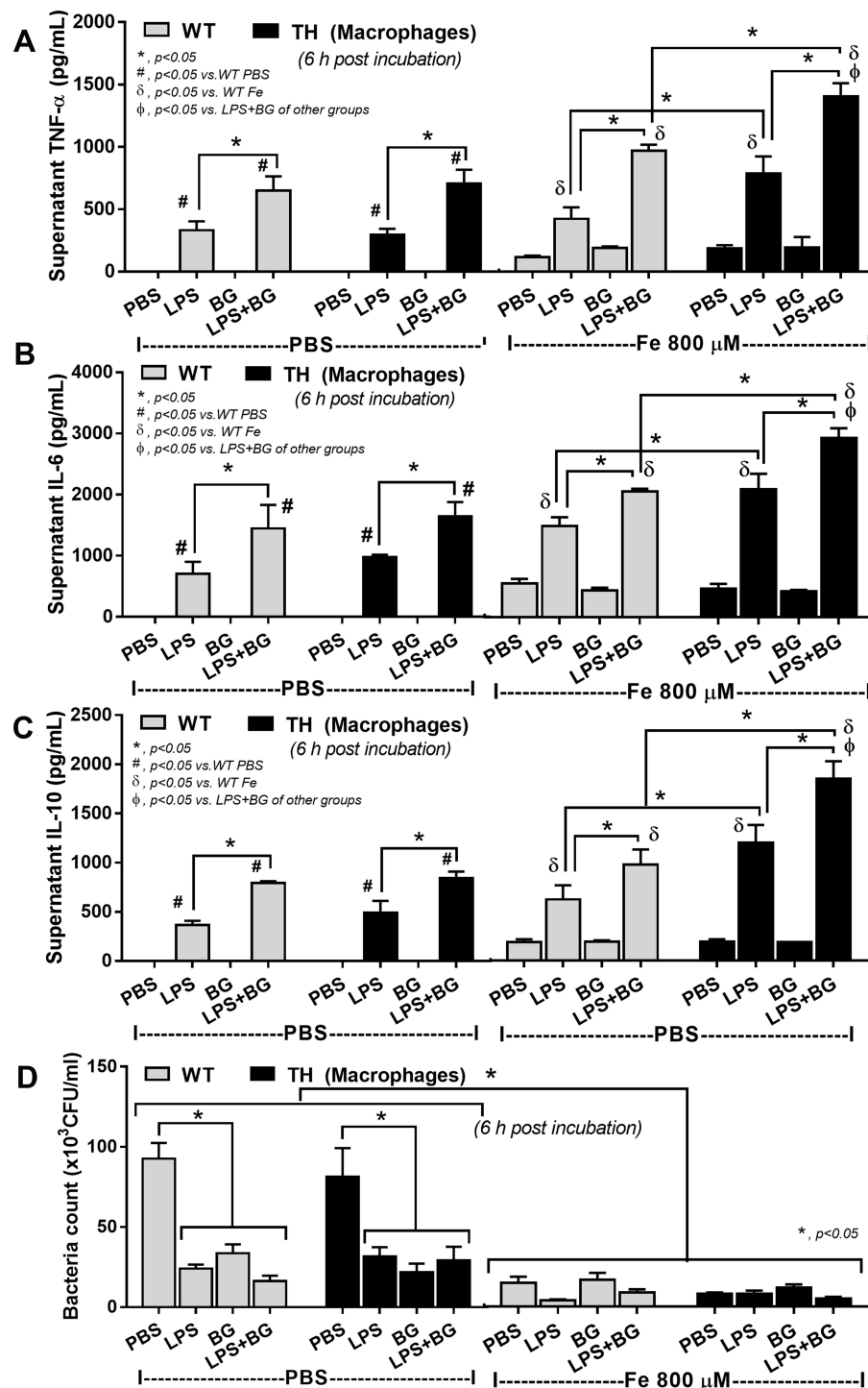


**Figure 5** Supernatant cytokines (A–C) and bactericidal activity (D) from bone marrow-derived macrophages of wild-type (WT) or thalassemia (TH) mice after 6 hours incubation with phosphate buffer solution (PBS), endotoxin (LPS), (1 $\rightarrow$ 3)- $\beta$ -D-glucan (BG) or LPS plus BG (LPS+BG) with or without ferric iron (800  $\mu$ M) are demonstrated (independent triplicated experiments were performed). \* $p < 0.05$ ; # $p < 0.05$  vs WT PBS;  $\delta$ ,  $p < 0.05$  vs WT Fe;  $\phi$ ,  $p < 0.05$  vs LPS+BG of other groups.

ion amplification effect, with the lower severity (Figure 6G–M) suggesting the higher impact of ferric ion upon LPS+BG over LPS alone. These data implied a limitation of energy reserve in pathogen-activated macrophages, especially in the iron-overload condition.

On the other hand, LPS+BG enhanced pro-inflammatory cytokines (TNF- $\alpha$  or IL-6) from neutrophils of both WT and TH groups compared with LPS alone and addition of ferric ion enhanced cytokine responses of LPS and LPS+BG in both cell types (Figure 7A and B).





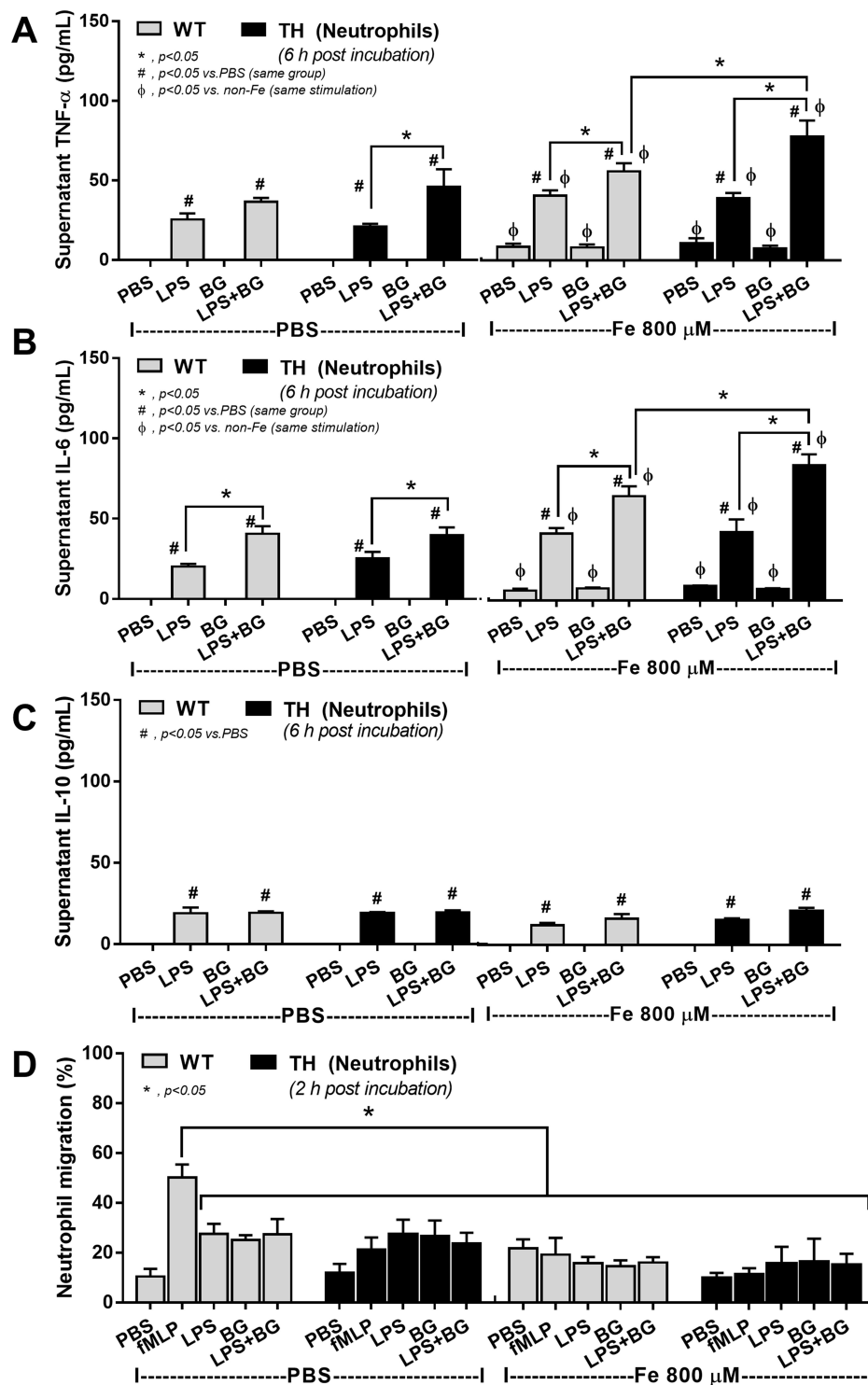


**Figure 7** Supernatant cytokines (A–C) from blood-derived neutrophils of wild-type (WT) or thalassemia (TH) mice after 6 hours incubation with phosphate buffer solution (PBS), endotoxin (LPS), (1 $\rightarrow$ 3)- $\beta$ -D-glucan (BG) or LPS plus BG (LPS+BG) with or without ferric iron (800  $\mu$ M) and neutrophil chemotactic activity (D) at 2 hour incubation of these parameters with chemotactic positive control by N-Formylmethionyl-leucyl-phenylalanine (fMLP) are demonstrated (independent triplicated experiments were performed). \* $p < 0.05$ ; # $p < 0.05$  vs PBS (same group);  $\phi$   $p < 0.05$  vs non-Fe (same stimulation).

However, the enhanced pro-inflammatory cytokine production was most prominent in LPS+BG activated TH neutrophils (Figure 7A and B). In parallel, supernatant IL-10 was not different between LPS vs LPS+BG,

regardless of ferric ion, in both WT and TH cells (Figure 7C). In addition, without ferric ion, there was a defect on neutrophil chemotaxis of TH neutrophils compared with WT cells (Figure 7D). With ferric ion, alone or in

combination with organismal molecules (LPS, BG or LPS +BG), WT neutrophils chemotaxis activity was reduced into the similar level of TH cells (Figure 7D). Of note, all activations did not further worsen chemotaxis of TH neutrophils (Figure 7D).

## Discussion

Iron overload induced more severe intestinal-barrier defects in TH mice compared with WT resulting in gut translocation of organismal molecules including LPS and BG from Gram negative bacteria and fungi, respectively, that worsened polymicrobial sepsis in TH mice through the pro-inflammatory activity.

### More Severe Gut Leakage-Induced Systemic Inflammation Increased Sepsis Susceptibility in Iron-Overload Thalassemia Mice

Excessive epithelium shedding, during iron elimination,<sup>50</sup> induces defective mucosal permeability, a single cell-layer barrier,<sup>11</sup> in 4 months iron-administered TH mice has been previously demonstrated.<sup>17</sup> Here, 6 month-iron administered TH mice induced gut leakage, similar to the previous studies,<sup>7,8,51</sup> and were susceptible to CLP sepsis in comparison with WT mice as determined by survival analysis and other parameters. Interestingly, without iron administration, sepsis severity in TH mice was not different to WT implying the non-prominent defect in immune response of TH mice. Iron toxicity in TH mice without sepsis (sham) was demonstrated by liver injury, gut leakage and systemic inflammation (TNF- $\alpha$  and IL-6) which was worsened by sepsis supporting the enhanced sepsis by pre-existing injury referred to as the “2 hits sepsis model.”<sup>14,15</sup> Hence, iron toxicity-induced systemic inflammation might be an important risk factor that enhances cytokine storm in sepsis<sup>19</sup> and iron with pathogen molecules from gut translocation might further worsen sepsis.

Accordingly, the severity of sepsis-induced neutropenia in WT and TH mice without iron overload was not different while, with iron overload, neutropenia in sepsis TH mice was more severe than WT. More severe neutropenia with higher monocyte count in iron-overload TH mice with sepsis compared with WT results in less effective organism-control with higher monocytes (or macrophages) cytokines production that enhanced sepsis severity.<sup>52,53</sup> Moreover, the defect of neutrophil maturation due to  $\beta$ -globin gene defect in TH mice without

sepsis is mentioned,<sup>30</sup> despite the similar neutrophil count from peripheral blood, this might also worsen sepsis in TH mice. In addition, the synergistic inflammatory effect of BG in exacerbation of LPS pro-inflammatory effects on immune cells in comparison with LPS activation alone is mentioned in several models.<sup>9,21–23</sup> The additive effect of the simultaneous stimulation of BG and LPS on Dectin-1 and TLR-4, respectively, is mentioned,<sup>26,30,54,55</sup> at least in part, due to the shared down-stream signaling, spleen tyrosine kinase (Syk), from both receptors.<sup>56,57</sup> However, the inflammatory responses of LPS plus BG (LPS+BG) with the presentation of iron have never been tested.

### The Synergistic Effect of Lipopolysaccharide (LPS) and (1 $\rightarrow$ 3)- $\beta$ -D-Glucan (BG) Upon Macrophages and Neutrophils

High dose of ferric ion (Fe<sup>3+</sup>), a less toxic oxidized trivalent-form than ferrous ion (Fe<sup>2+</sup>), that is systemically transported in the body,<sup>58</sup> was used in the in vitro experiment.

While LPS and BG (alone or in combination) similarly enhanced macrophage bactericidal activity without synergy, the additive effect of BG upon LPS in cytokine production and M1 macrophage polarization was demonstrated in both WT and TH macrophages. Interestingly, ferric ion enhanced cytokine production and M1 macrophage polarization of LPS or LPS+BG more predominantly in TH macrophages in comparison with WT cells supporting the iron-enhanced M1 macrophage polarization as previously mentioned.<sup>43</sup> Since 1) M1 macrophage polarization associates with hyper-inflammatory state and cytokine storm in sepsis,<sup>53</sup> and 2) reduction of M1 macrophage polarization attenuates sepsis severity,<sup>59</sup> severe sepsis in iron-overload TH mice, at least in part, may be due to the increased M1 polarization. Although BG alone did not induce macrophage inflammation, BG together with LPS and ferric ion induced a potent additive effect on cytokine production in TH macrophages implying an important role of iron-overload in pro-inflammatory responses of TH mice.

Moreover, LPS+BG or LPS alone reduced respiratory capacity (mitochondrial function) but enhanced glycolysis activity, an energy production process that associated with macrophage cytokine production, in comparison with the control group.<sup>60</sup> Furthermore, respiratory capacity

(mitochondrial function), but not glycolysis activity, was worse in LPS or LPS+BG with ferric iron possibly due to iron toxicity-related mitochondrial DNA damage.<sup>61</sup> Because energy production by respiratory capacity is more effective than glycolysis, decreased mitochondrial activity after LPS+BG activation demonstrated cell-energy defect that is vulnerable to cell stresses.<sup>62</sup> In neutrophils, LPS+BG also induced higher cytokine production (TNF- $\alpha$  and IL-6) compared with LPS alone in both WT and TH but ferric ion predominantly enhanced the function of TH cells. On the other hand, neutrophil chemotaxis activity of TH cells was lower than WT cells and ferric ion, LPS or BG, alone or in combination, similarly reduced chemotaxis activity in both groups. These data are supported by the predominant impact of serum BG in iron-overload TH mice in enhancing responses of innate immune cells (macrophages and neutrophils) that accelerated cytokine storm in CLP sepsis. However, the other mediators and the adaptive immunity might be also important in sepsis of TH mice such as IL-33, a cytokine originally described as an adaptive immunity molecule, which enhances the neutrophil influx to the site of infection during sepsis.<sup>63,64</sup> More studies are interesting.

Hence, mildly pre-existing inflammatory state in iron-overload TH<sup>65</sup> was, at least in part, responsible for gut translocation of organismal molecules including LPS and BG, a major cell wall component of Gram-negative bacteria and fungi, respectively. Manipulation of gut organisms or organismal molecules, in gut contents or in serum, and biomarkers of inflammation and gut leakage might be beneficial for patients with TH and sepsis. Although oral anti-microbial agents might reduce organism burdens in gut, the existing organisms with higher virulence could worsen the model. Future studies with the appropriate strategies are warranted.

In conclusion, gut-leakage-induced spontaneous gut translocation of organismal molecules in iron-overload TH mice induced an inflammatory status through the activation on macrophages and neutrophils that is susceptible to sepsis.

## Funding

This study was supported by Thailand Government Fund (RSA-6080023), Thailand Research Fund (RES\_61\_20\_2\_30\_022) and Ratchadaphiseksomphot Endowment Fund 2017 (76001-HR).

## Disclosure

The authors report no conflicts of interest in this work.

## References

1. Fucharoen S, Winichagoon P. New updating into hemoglobinopathies. *Int J Lab Hematol*. 2012;34(6):559–565. doi:10.1111/j.1751-553X.2012.01446.x
2. Rivella S. Ineffective erythropoiesis and thalassemias. *Curr Opin Hematol*. 2009;16(3):187–194. doi:10.1097/MOH.0b013e32832990a4
3. Rachmilewitz EA, Giardina PJ. How I treat thalassemia. *Blood*. 2011;118(13):3479–3488. doi:10.1182/blood-2010-08-300335
4. Taher AT, Saliba AN. Iron overload in thalassemia: different organs at different rates. *Hematology Am Soc Hematol Educ Program*. 2017;2017(1):265–271. doi:10.1182/asheducation-2017.1.265
5. Khan FA, Fisher MA, Khakoo RA. Association of hemochromatosis with infectious diseases: expanding spectrum. *Int J Infect Dis*. 2007;11(6):482–487. doi:10.1016/j.ijid.2007.04.007
6. Moura E, Noordermeer MA, Verhoeven N, Verheul AF, Marx JJ. Iron release from human monocytes after erythrophagocytosis in vitro: an investigation in normal subjects and hereditary hemochromatosis patients. *Blood*. 1998;92(7):2511–2519. doi:10.1182/blood.V92.7.2511
7. Fang S, Yu X, Ding H, Han J, Feng J. Effects of intracellular iron overload on cell death and identification of potent cell death inhibitors. *Biochem Biophys Res Commun*. 2018;503(1):297–303. doi:10.1016/j.bbrc.2018.06.019
8. Fang S, Zhuo Z, Yu X, Wang H, Feng J. Oral administration of liquid iron preparation containing excess iron induces intestine and liver injury, impairs intestinal barrier function and alters the gut microbiota in rats. *J Trace Elem Med Biol*. 2018;47:12–20. doi:10.1016/j.jtemb.2018.01.002
9. Issara-Amphorn J, Surawut S, Worasilchai N, et al. The synergy of endotoxin and (1 $\rightarrow$ 3)-beta-D-glucan, from gut translocation, worsens sepsis severity in a lupus model of Fc gamma receptor IIb-deficient mice. *J Innate Immun*. 2018;10(3):189–201. doi:10.1159/000486321
10. Panpetch W, Chanchaoentana W, Bootdee K, et al. Lactobacillus rhamnosus L34 attenuates gut translocation-induced bacterial sepsis in murine models of leaky gut. *Infect Immun*. 2018;86(1):e00700–e00717.
11. Amornphimoltham P, Yuen PST, Star RA, Leelahavanichkul A. Gut leakage of fungal-derived inflammatory mediators: part of a gut-liver-kidney axis in bacterial sepsis. *Dig Dis Sci*. 2019;64(9):2416–2428. doi:10.1007/s10620-019-05581-y
12. Teawtrakul N, Jetsrisuparb A, Sirirerachai C, Chansung K, Wanitpongpan C. Severe bacterial infections in patients with non-transfusion-dependent thalassemia: prevalence and clinical risk factors. *Int J Infect Dis*. 2015;39:53–56. doi:10.1016/j.ijid.2015.09.001
13. Vento S, Cainelli F, Cesario F. Infections and thalassaemia. *Lancet Infect Dis*. 2006;6(4):226–233. doi:10.1016/S1473-3099(06)70437-6
14. Doi K, Leelahavanichkul A, Hu X, et al. Pre-existing renal disease promotes sepsis-induced acute kidney injury and worsens outcome. *Kidney Int*. 2008;74(8):1017–1025. doi:10.1038/ki.2008.346
15. Leelahavanichkul A, Huang Y, Hu X, et al. Chronic kidney disease worsens sepsis and sepsis-induced acute kidney injury by releasing high mobility group box protein-1. *Kidney Int*. 2011;80(11):1198–1211. doi:10.1038/ki.2011.261
16. Odeberg J, Freitag M, Forsell H, et al. Influence of pre-existing inflammation on the outcome of acute coronary syndrome: a cross-sectional study. *BMJ Open*. 2016;6(1):e009968.
17. Visitchanakun P, Saisorn W, Wongphoom J, et al. Gut leakage enhances sepsis susceptibility in iron-overloaded  $\beta$ -thalassemia mice through macrophage hyperinflammatory responses. *Am J Physiol Gastrointest Liver Physiol*. 2020;318(5):G966–G979. doi:10.1152/ajpgi.00337.2019

18. Seemann S, Zohles F, Lupp A. Comprehensive comparison of three different animal models for systemic inflammation. *J Biomed Sci.* 2017;24(1):60. doi:10.1186/s12929-017-0370-8
19. Doi K, Leelahavanichkul A, Yuen PS, Star RA. Animal models of sepsis and sepsis-induced kidney injury. *J Clin Invest.* 2009;119(10):2868–2878. doi:10.1172/JCI39421
20. Wen H. Sepsis induced by cecal ligation and puncture. In: *Mouse Models of Innate Immunity*. Springer; 2013:117–124.
21. Panpetch W, Somboonna N, Bulan DE, et al. Oral administration of live-or heat-killed *Candida albicans* worsened cecal ligation and puncture sepsis in a murine model possibly due to an increased serum (1→3)-β-D-glucan. *PLoS One.* 2017;12(7):e0181439. doi:10.1371/journal.pone.0181439
22. Panpetch W, Hiengrach P, Nilgate S, et al. Additional *Candida albicans* administration enhances the severity of dextran sulfate solution induced colitis mouse model through leaky gut-enhanced systemic inflammation and gut-dysbiosis but attenuated by *Lactobacillus rhamnosus* L34. *Gut Microbes.* 2019;1–16.
23. Thim-Uam A, Surawut S, Issara-Amphorn J, et al. Leaky-gut enhanced lupus progression in the Fc gamma receptor-IIb deficient and pristane-induced mouse models of lupus. *Sci Rep.* 2020;10(1):777. doi:10.1038/s41598-019-57275-0
24. Koh AY. Murine models of *Candida* gastrointestinal colonization and dissemination. *Eukaryot Cell.* 2013;12(11):1416–1422. doi:10.1128/EC.00196-13
25. Yang AM, Inamine T, Hochrath K, et al. Intestinal fungi contribute to development of alcoholic liver disease. *J Clin Invest.* 2017;127(7):2829–2841. doi:10.1172/JCI90562
26. Ferwerda G, Meyer-Wentrop F, Kullberg BJ, Netea MG, Adema GJ. Dectin-1 synergizes with TLR2 and TLR4 for cytokine production in human primary monocytes and macrophages. *Cell Microbiol.* 2008;10(10):2058–2066. doi:10.1111/j.1462-5822.2008.01188.x
27. Engstad CS, Engstad RE, Olsen JO, Osterud B. The effect of soluble beta-1,3-glucan and lipopolysaccharide on cytokine production and coagulation activation in whole blood. *Int Immunopharmacol.* 2002;2(11):1585–1597. doi:10.1016/S1567-5769(02)00134-0
28. Liu L, Zeng M, Stamler JS. Hemoglobin induction in mouse macrophages. *Proc Natl Acad Sci U S A.* 1999;96(12):6643–6647. doi:10.1073/pnas.96.12.6643
29. Saha D, Patgaonkar M, Shroff A, Ayyar K, Bashir T, Reddy KV. Hemoglobin expression in nonerythroid cells: novel or ubiquitous? *Int J Inflam.* 2014;2014:803237. doi:10.1155/2014/803237
30. Siwaponnan P, Siegers JY, Ghazali R, et al. Reduced PU.1 expression underlies aberrant neutrophil maturation and function in β-thalassemia mice and patients. *Blood.* 2017;129(23):3087–3099. doi:10.1182/blood-2016-07-730135
31. Vu CTB, Thammahong A, Yagita H, et al. Blockade of PD-1 attenuated postsepsis aspergillosis via the activation of IFN-gamma and the dampening of IL-10. *Shock.* 2020;53(4):514–524. doi:10.1097/SHK.0000000000001392
32. Visitchanakun P, Tangtanatakul P, Trithiphen O, et al. Plasma miR-370-3p as a biomarker of sepsis-associated encephalopathy, the transcriptomic profiling analysis of microRNA-arrays from mouse brains. *Shock (Augusta, Ga).* 2019.
33. Leelahavanichkul A, Sompam P, Bootprapan T, et al. High-dose ascorbate with low-dose amphotericin B attenuates severity of disease in a model of the reappearance of candidemia during sepsis in the mouse. *Am J Physiol Regul Integr Comp Physiol.* 2015;309(3):R223–R234.
34. Leelahavanichkul A, Worasilchai N, Wannalerdsakun S, et al. Gastrointestinal leakage detected by serum (1→3)-beta-D-glucan in mouse models and a pilot study in patients with sepsis. *Shock.* 2016;46(5):506–518. doi:10.1097/SHK.0000000000000645
35. Scupham AJ, Presley LL, Wei B, et al. Abundant and diverse fungal microbiota in the murine intestine. *Appl Environ Microbiol.* 2006;72(1):793–801. doi:10.1128/AEM.72.1.793-801.2006
36. Rowatt K, Burns RE, Frasca S, Long DM. A combination Prussian blue – hematoxylin and eosin staining technique for identification of iron and other histological features. *J Histotechnol.* 2018;41(1):29–34. doi:10.1080/01478885.2017.1417696
37. Leelahavanichkul A, Yasuda H, Doi K, et al. Methyl-2-acetamidocrylate, an ethyl pyruvate analog, decreases sepsis-induced acute kidney injury in mice. *Am J Physiol Renal Physiol.* 2008;295(6):F1825–F1835. doi:10.1152/ajprenal.90442.2008
38. Suzuki S, Toledopereyra LH, Rodriguez FJ, Cejalvo D. Neutrophil infiltration as an important factor in liver ischemia and reperfusion injury - modulating effects of Fk506 and cyclosporine. *Transplantation.* 1993;55(6):1265–1272. doi:10.1097/00007890-199306000-00011
39. Garofalo AM, Lorente-Ros M, Goncalvez G, et al. Histopathological changes of organ dysfunction in sepsis. *Intensive Care Med Exp.* 2019;7(Suppl 1):45. doi:10.1186/s40635-019-0236-3
40. Panpetch W, Somboonna N, Bulan DE, et al. Gastrointestinal colonization of *Candida albicans* increases serum (1→3)-β-D-glucan, without candidemia, and worsens cecal ligation and puncture sepsis in murine model. *Shock.* 2018;49(1):62–70.
41. Ondee T, Jaroowitchawan T, Pisitkun T, et al. Decreased protein kinase C-β Type II associated with the prominent endotoxin exhaustion in the macrophage of FcγRIIb-/- lupus prone mice is revealed by phosphoproteomic analysis. *Int J Mol Sci.* 2019;20(6):1354. doi:10.3390/ijms20061354
42. Surawut S, Ondee T, Taratummarat S, et al. The role of macrophages in the susceptibility of Fc gamma receptor IIb deficient mice to *Cryptococcus neoformans*. *Sci Rep.* 2017;7(1):40006. doi:10.1038/srep40006
43. Zhou Y, Que KT, Zhang Z, et al. Iron overloaded polarizes macrophage to proinflammation phenotype through ROS/acetyl-p53 pathway. *Cancer Med.* 2018;7(8):4012–4022. doi:10.1002/cam4.1670
44. Nemeth E, Ganz T. Regulation of iron metabolism by hepcidin. *Annu Rev Nutr.* 2006;26:323–342. doi:10.1146/annurev.nutr.26.061505.111303
45. Chiewchengechol D, Wright HL, Thomas HB, et al. Differential changes in gene expression in human neutrophils following TNF-α stimulation: up-regulation of anti-apoptotic proteins and down-regulation of proteins involved in death receptor signaling. *Immun Inflam Dis.* 2016;4(1):35–44. doi:10.1002/iid3.90
46. Hu Y. Isolation of human and mouse neutrophils ex vivo and in vitro. In: *Leucocytes*. Springer; 2012:101–113.
47. Sae-Khow K, Tachaboon S, Wright HL, et al. Defective neutrophil function in patients with sepsis is mostly restored by ex vivo ascorbate incubation. *J Inflamm Res.* 2020;13:263–274. doi:10.2147/JIR.S252433
48. Hiengrach P, Panpetch W, Worasilchai N, et al. Administration of *Candida albicans* to dextran sulfate solution treated mice causes intestinal dysbiosis, emergence and dissemination of intestinal *Pseudomonas aeruginosa* and lethal sepsis. *Shock.* 2019.
49. Liu YC, Zou XB, Chai YF, Yao YM. Macrophage polarization in inflammatory diseases. *Int J Biol Sci.* 2014;10(5):520–529. doi:10.7150/ijbs.8879
50. Williams JM, Duckworth CA, Burkitt MD, Watson AJM, Campbell BJ, Pritchard DM. Epithelial cell shedding and barrier function: a matter of life and death at the small intestinal villus tip. *Vet Pathol.* 2015;52(3):445–455. doi:10.1177/0300985814559404
51. Eid R, Arab NT, Greenwood MT. Iron mediated toxicity and programmed cell death: a review and a re-examination of existing paradigms. *Biochim Biophys Acta Mol Cell Res.* 2017;1864(2):399–430. doi:10.1016/j.bbamer.2016.12.002
52. Sonogo F, Castanheira FV, Ferreira RG, et al. Paradoxical roles of the neutrophil in sepsis: protective and deleterious. *Front Immunol.* 2016;7:155. doi:10.3389/fimmu.2016.00155



53. Hamidzadeh K, Christensen SM, Dalby E, Chandrasekaran P, Mosser DM. Macrophages and the recovery from acute and chronic inflammation. *Annu Rev Physiol.* 2017;79:567–592. doi:10.1146/annurev-physiol-022516-034348
54. Dennehy KM, Ferwerda G, Faro-Trindade I, et al. Syk kinase is required for collaborative cytokine production induced through Dectin-1 and Toll-like receptors. *Eur J Immunol.* 2008;38(2):500–506. doi:10.1002/eji.200737741
55. Kikkert R, Bulder I, de Groot ER, Aarden LA, Finkelman MA. Potentiation of Toll-like receptor-induced cytokine production by (1→3)-beta-D-glucans: implications for the monocyte activation test. *J Endotoxin Res.* 2007;13(3):140–149. doi:10.1177/0968051907080024
56. Issara-Amphorn J, Somboonna N, Pisitkun P, Hirankarn N, Leelahavanichkul A. Syk inhibitor attenuates inflammation in lupus mice from FcγRIIb deficiency but not in pristane induction: the influence of lupus pathogenesis on the therapeutic effect. *Lupus.* 2020;29(10):1248–1262. doi:10.1177/0961203320941106
57. Yi YS, Son YJ, Ryou C, Sung GH, Kim JH, Cho JY. Functional roles of Syk in macrophage-mediated inflammatory responses. *Mediators Inflamm.* 2014;2014:270302. doi:10.1155/2014/270302
58. Sukhbaatar N, Weichhart T. Iron regulation: macrophages in control. *Pharmaceuticals (Basel).* 2018;11(4):137. doi:10.3390/ph11040137
59. Dang CP, Leelahavanichkul A. Over-expression of miR-223 induces M2 macrophage through glycolysis alteration and attenuates LPS-induced sepsis mouse model, the cell-based therapy in sepsis. *PLoS One.* 2020;15(7):e0236038. doi:10.1371/journal.pone.0236038
60. Thapa B, Lee K. Metabolic influence on macrophage polarization and pathogenesis. *BMB Rep.* 2019;52(6):360–372. doi:10.5483/BMBRep.2019.52.6.140
61. Walter PB, Knutson MD, Paler-Martinez A, et al. Iron deficiency and iron excess damage mitochondria and mitochondrial DNA in rats. *Proc Natl Acad Sci U S A.* 2002;99(4):2264–2269. doi:10.1073/pnas.261708798
62. Picard M, McEwen BS, Epel ES, Sandi C. An energetic view of stress: focus on mitochondria. *Front Neuroendocrinol.* 2018;49:72–85. doi:10.1016/j.yfrne.2018.01.001
63. Alves-Filho JC, Sonego F, Souto FO, et al. Interleukin-33 attenuates sepsis by enhancing neutrophil influx to the site of infection. *Nat Med.* 2010;16(6):708–712. doi:10.1038/nm.2156
64. Liew FY, Girard JP, Turnquist HR. Interleukin-33 in health and disease. *Nat Rev Immunol.* 2016;16(11):676–689. doi:10.1038/nri.2016.95
65. Wanachiwanawin W, Wiener E, Siripanyaphinyo U, et al. Serum levels of tumor necrosis factor-alpha, interleukin-1, and interferon-gamma in beta-thalassemia/HbE and their clinical significance. *J Interferon Cytokine Res.* 1999;19(2):105–111. doi:10.1089/107999099314243

## Journal of Inflammation Research

### Publish your work in this journal

The Journal of Inflammation Research is an international, peer-reviewed open-access journal that welcomes laboratory and clinical findings on the molecular basis, cell biology and pharmacology of inflammation including original research, reviews, symposium reports, hypothesis formation and commentaries on: acute/chronic inflammation; mediators of inflammation; cellular processes; molecular

mechanisms; pharmacology and novel anti-inflammatory drugs; clinical conditions involving inflammation. The manuscript management system is completely online and includes a very quick and fair peer-review system. Visit <http://www.dovepress.com/testimonials.php> to read real quotes from published authors.

Submit your manuscript here: <https://www.dovepress.com/journal-of-inflammation-research-journal>

Dovepress